



Can Apparent Diffusion Coefficient (ADC) maps replace Diffusion Tensor Imaging (DTI) maps to predict the volumetric response of meningiomas to Gamma Knife Radiosurgery?

Herwin Speckter^{1,2} · Sarai Palque-Santos¹ · Ruben Mota-Gonzalez¹ · Jose Bido¹ · Giancarlo Hernandez¹ · Diones Rivera¹ · Luis Suazo¹ · Santiago Valenzuela¹ · Maria Gonzalez-Curi² · Peter Stoeter^{1,2}

Received: 22 December 2022 / Accepted: 17 January 2023 / Published online: 6 February 2023
© The Author(s), under exclusive licence to Springer Science+Business Media, LLC, part of Springer Nature 2023

Abstract

Purpose Noninvasive methods are desired to predict the treatment response to Stereotactic Radiosurgery (SRS) to improve individual tumor management. In a previous study, we demonstrated that Diffusion Tensor Imaging (DTI)-derived parameter maps significantly correlate to SRS response. This study aimed to analyze and compare the predictive value of intratumoral ADC and DTI parameters in patients with meningiomas undergoing radiosurgery.

Methods MR images of 70 patients treated with Gamma Knife SRS for WHO grade I meningiomas were retrospectively reviewed. MR acquisition included pre- and post-treatment DWI and DTI sequences, and subtractions were calculated to assess for radiation-induced changes in the parameter values.

Results After a mean follow-up period (FUP) of 52.7 months, 69 of 70 meningiomas were controlled, with a mean volume reduction of 34.9%. Whereas fractional anisotropy (FA) values of the initial exam showed the highest correlation to tumor volume change at the last FU ($CC = -0.607$), followed by the differences between first and second FU values of FA ($CC = -0.404$) and the first longitudinal diffusivity (LD) value ($CC = -0.375$), the correlation coefficients of all ADC values were comparably low. Nevertheless, all these correlations, except for ADC measured at the first follow-up, reached significance.

Conclusion For the first time, the prognostic value of ADC maps measured in meningiomas before and at first follow-up after Gamma Knife SRS, was compared to simultaneously acquired DTI parameter maps. Quantities assessed from ADC maps present significant correlations to the volumetric meningioma response but are less effective than correlations with DTI parameters.

Keywords Radiosurgery · Meningioma · Volumetric response · Apparent Diffusion Coefficient · Diffusion Tensor Imaging · Outcome prediction

✉ Herwin Speckter
hspeckter@cedimat.net

Sarai Palque-Santos
sp15-1929@unphu.edu.do

Ruben Mota-Gonzalez
emiliomota97@gmail.com

Jose Bido
Josebido1@yahoo.com

Giancarlo Hernandez
neurogh@hotmail.com

Diones Rivera
dionesrivera@gmail.com

Luis Suazo
lsuazo@cedimat.net

Santiago Valenzuela
stgo.sosa@gmail.com

Maria Gonzalez-Curi
Migonzalez@cedimat.net

Peter Stoeter
Peter.stoeter@gmx.de

¹ Centro Gamma Knife Dominicano, CEDIMAT, Plaza de la Salud, Santo Domingo, Dominican Republic

² Department of Radiology, CEDIMAT, Plaza de la Salud, Santo Domingo, Dominican Republic

Introduction

Even though Stereotactic Radiosurgery (SRS) has proven a control rate of up to more than 95% in the treatment of meningiomas [1–4] there are still some failures. In large-volume tumors, the control rate may be as low as 84% and even below 70% in atypical and anaplastic types, accompanied by increased radiation-induced toxicity up to 23% [5, 6]. The search for prognostic parameters to support the treatment decision-making process appears to be justified.

In addition to clinical symptoms and parameters such as age, general health, neurologic deficit, and recurrence after previous treatment, tumor size and localization have served as prognostic indicators [7–12]. Diffusion Weighted Imaging (DWI) and Diffusion Tensor Imaging (DTI) parameters were also applied to predict meningioma type, consistency, and grading, including texture analysis and machine learning techniques [13–19].

In a previous analysis of Magnetic Resonance Imaging (MRI) data measured before SRS, several DTI parameter maps, particularly Fraction Anisotropy (FA) values, correlated strongly to treatment outcome [20]. We hypothesized that different subtypes of meningiomas respond differently to SRS. The lower responsiveness of fiber-rich tissue to radiation, as it is found in fibrous subtypes, is a well-known fact in radiation therapy [20].

However, DTI parameters are only measured occasionally for SRS treatment planning. As a replacement, Apparent Diffusion Coefficient (ADC) maps from simple DWI have been suggested [21]. In a previous first-level texture analysis of DTI parameters of meningiomas before SRS, we were able to show that mean diffusivity (MD), which is a DTI parameter comparable to ADC, indeed correlated significantly to volume regression [22].

The present retrospective study was carried out to investigate if the application of a standard DWI sequence could give similar prognostic results as pattern analysis of DTI parameters, as DTI is not routinely included in the imaging protocol of brain tumors planned for SRS.

Patients and methods

This retrospective study had been approved by the institutional review board at our institution and informed consent was obtained from all individual participants included in the study.

Patients and meningiomas

Included into the retrospective study were 70 patients between 27 and 81 (mean 56) years of age, who had been diagnosed as carriers of an intracranial low-grade meningioma and had been treated by SRS at our Gamma Knife center. Pre-operated cases with a histologic diagnosis of a higher grade than grade 1 were excluded as well as cases with multifocal lesions. Further inclusion criteria were a pre-treatment MRI measured during the last two months before SRS, an “early” follow-up (FU) MRI approximately 6 months after SRS to examine changes of diffusion parameters, and a late FU MRI after a period of 18 months or more to assess for tumor response after SRS. MRI images with obvious movement or susceptibility artifacts were excluded. MR acquisition included pre- and post-treatment DWI and DTI sequences, to allow for subtractions to assess for radiation-induced changes of the parameter values.

We were able to retrieve histology results from 9 of 33 cases in which a preceding operation was documented. All operated cases followed subtotal resection; no recurrent meningioma was included to this study. Six of the tumors were characterized as meningothelial and psammomatous meningioma, three as a fibroblastic subtype, all without atypical features. 61 remaining cases without known histology were assigned as WHO grade I, based on criteria such as homogeneously enhancing, dural tails, no extension through cranial foramina, no substantial peritumoral edema, no significant lobulations [23]. 58 meningiomas (83%) were localized at the cranial base, most of them in the cranial fossa, 9 meningiomas were localized at the convexity, and 3 meningiomas were localized at the tentorium.

MRI had been performed within 2 months before their GKRS, and follow-up data from at least one early FU MR scan (range 2.4–15.2 months, mean 7.2 months) and one late FU MR scan (range 17.0–108.1 months, mean 52.7 months) were available (Table 1).

Gamma Knife treatment

All treatment were performed using a Gamma Knife model 4C (Elekta AB, Stockholm, Sweden). Details of the GKRS treatment technique were previously described [24], with the exception that at our center, MRI images were acquired up to 2 months before treatment. On treatment day, after placement of a stereotactic G frame (Elekta AB), MRI sequences were coregistered to the stereotactic contrast-enhanced 3D CT image set.

Table 1 Patients and treatment characteristics

Patient and treatment characteristics	Value	Range
Number of patients	70	–
Age in years (mean, range)	55.8	(26.6/81.3)
Pre-SRS tumor volume in cm ³ (mean, range)	9.58	(0.62/33.09)
Previous RT, SRS	0	–
Previous surgery	33	–
KPS before SRS	90.6	(60 / 100)
Single fraction SRS treatments	63	–
Hypofractionated SRS treatments	7	–
Number of fractions (mean, range)	1.29	(1/4)
Coverage index (mean, range)	96.6%	(87.0%/99.0%)
Selectivity index (mean, range)	66.0%	(17.0%/91.0%)
Paddick conformity index (mean, range)	63.8	(16.8/88.3)
Number of isocenters (mean, range)	7.3	(1/29)
Margin physical dose in Gy (mean, range)	14.4	(11/20)
Maximum physical dose in Gy (mean, range)	28.8	(22/40)
Margin BED in Gy (mean, range)	63.1	(43.2/104.2)
Margin SFED in Gy (mean, range)	13.5	(11.0/18.0)

SRS stereotactic radiosurgery, RT radiotherapy, GK gamma knife, BED biologically effective dose, SFED single fraction equivalent dose

Depending on tumor size and localization, the margin dose varied from 11 to 20 Gy (Table 1). Sixty-three meningiomas were treated in a single session, with margin doses between 11 and 18 Gy (mean 13.8 Gy). According to our institutional protocol, meningioma abutting organs at risk, particularly the anterior optic pathway, were treated using hypofractionated radiosurgery (HFSRS). This was the case for seven meningiomas that were treated with an application of 6 Gy for 3 consecutive days or of 5 Gy during 4 successive days. During hypofractionated courses, the stereotactic frame was left on the patient's head. Daily low-dose CT acquisitions assured accurate frame location during the treatment period, and all patients tolerated the procedure well. Biologically effective dose (BED) is routinely used to compare doses of different dose-fraction regimens, based on the widely accepted linear quadratic (LQ) model, although with its limitations for high doses still in debate [25]. HFSRS doses can be converted to single fraction equivalent doses (SFED), [26] to intuitively compare radiation effects to conventional physical doses of single fraction radiosurgery. Margin SFED of the seven HFSRS treatments was on average 11.5 Gy, applying an α/β ratio of 3.76 Gy [27]. Treatments were planned on a Leksell GammaPlan 10.1 workstation (Elekta AB, Stockholm, Sweden), by optimizing tumor coverage (mean 96.6%), while restricting doses to sensitive structures, such as the optic apparatus, the cochlea, or the brainstem.

Magnetic Resonance Imaging

MRI was performed on a 3-Tesla scanner (Achieva; Philips, Eindhoven, Netherlands). The following sequences were applied:

- 1) 3D T1 magnetization-prepared rapid acquisition (MPRAGE) sequence: gradient echo, TR/TE/TI 6.8/3.2/900 ms, flip angle 8°, measured voxel size 0.6*0.6*1.0 mm, before and after intravenous injection of contrast medium.
- 2) T2-weighted sequence: TR/TE 3693.8/80 ms, 150 transversal slices, thickness 1 mm, matrix 512×512.
- 3) Fluid-attenuated inversion recovery (FLAIR) sequence: TR/TE/TI 11,000/120/2800 ms, 90 transversal slices, thickness 2 mm, matrix 512×512.
- 4) DWI spin echo-based fat sat 2D sequence: TR/TE 2445/70 ms, flip angle 90°, b-factor 0 and 1000 s/mm², 3 gradient directions, measured voxel size 0.9×0.9×5 mm, 25 slices covering whole head, SENSE factor 2, scanning time 29.3 s.
- 5) DTI spin echo-based fat-sat 2D sequence: TR/TE=6542/60 ms, flip angle 90°, 32 gradient directions, b=0 and 800 mm²/s, measured voxel size 2×2×2mm, 60 slices covering the whole head, SENSE factor 2, scanning time 4.5 min

DTI and DWI sequences differ with respect to slice thickness and voxel size. Therefore, the DWI sequence is more prone to partial volume averaging than the DTI dataset. Special care was taken to exclude bones, CSF spaces, and vascular structures in a similar way in both sequences.

Postprocessing

Tumor volumes were outlined manually and measured from 3D T1-weighted contrast-enhanced images on the Leksell GammaPlan workstation. Dural tails were not included in the tumor volume, as these are commonly kept out of the treatment volume in radiosurgery [28]. The volumetric outcome was classified according to RANO criteria for meningiomas, which divides response into five types based on T1-weighted images after injection of contrast media [29] (Table 2). In case of DWI images, the “MRIcro” program (people.cas.sc.edu/rorden/mricro) was used for tumor delineation, and special care was taken to exclude CSF/containing and bone containing spaces outside the meningioma as well as big vessels passing the tumor as in parasellar growths. Thus, average ADC values could be measured directly from d-maps and were recorded voxel-wise. DTI data were transferred into the “ExploreDTI” program (<http://exploredti.com>). Images were corrected for motion artifacts and maps of Fractional Anisotropy (FA), Mean Diffusivity (MD),

Table 2 Treatment results

Treatment results	Value	Range
Delay to first MRI FU in months (mean, range)	7.2	(2.4/15.2)
Delay to last MRI FU in months (mean, range)	52.7	(17.0/108.1)
Complete response (disappearance)	0 [0%]	–
Partial response ($\geq 50\%$ decrease, no disappearance)	17 [24.3%]	–
Minor response ($\geq 25\%$ and $< 50\%$ decrease)	29 [41.4%]	–
Stable disease ($< 25\%$ decrease, but $< 25\%$ increase)	23 [32.9%]	–
Progressive disease ($\geq 25\%$ increase)	1 [1.4%]	–
Control rate	98.6%	
Absolute volume change in cm ³ (mean, range)	– 3.17	(– 16.91/5.75)
Relative volume change (mean, range)	– 34.94%	(– 91.4%/73.1%)
Volume change per month (mean, range)	– 0.77%	(– 3.16%/0.68%)
Volume change per ln(month) (mean, range)	– 0.209	(– 0.626/0.360)

FU follow up

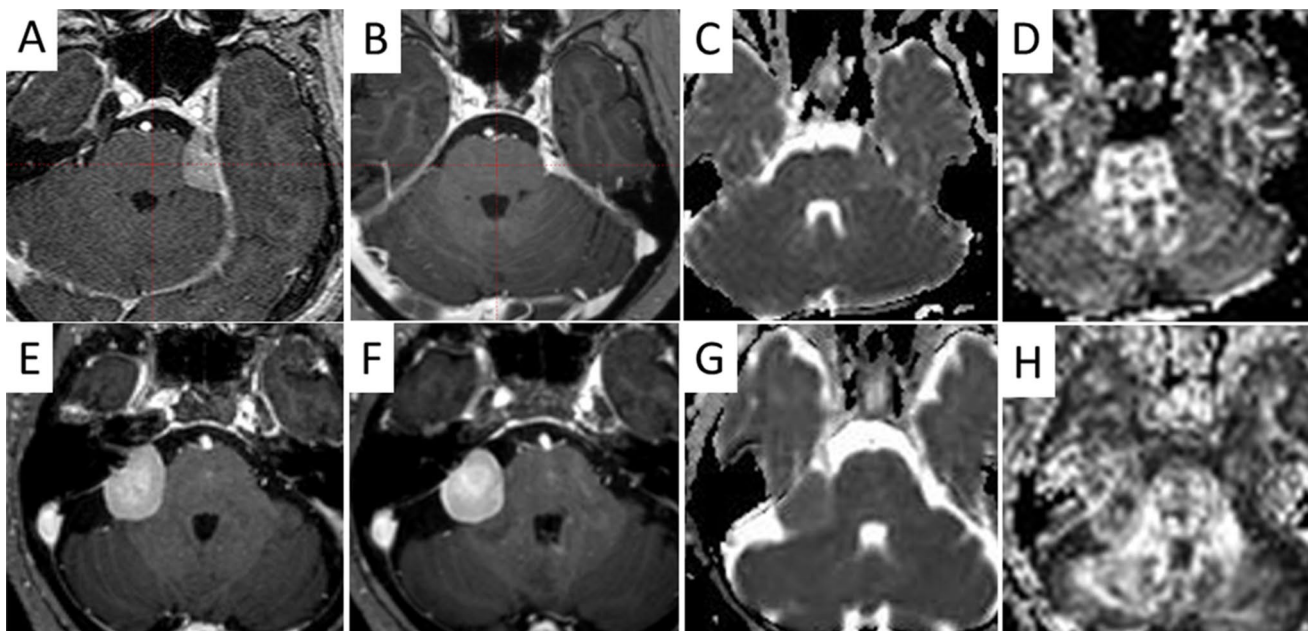


Fig. 1 A–D: A 52-year-old female patient with a posterior fossa meningioma. Contrast-enhanced, T1-weighted MRI, ADC-map, FA-map. Before GKRS (Fig. 1A), the volume was 3.34 cm³. An 80% reduction in volume was noted at 87 months after GKRS (remained volume 0.655 cm³), regression rate of 0.93%/m (Fig. 1B). ADC value of 802×10^{-6} mm²/s (Fig. 1C), very low FA value of 0.145 (Fig. 1D).

E–H: A 77-year-old female patient with a posterior fossa meningioma. Contrast-enhanced, T1-weighted MRI, ADC-map, FA-map. Before GKRS, the volume was 5.24 cm³ (Fig. 1E). An increase of 6.7% in volume was noted at 38 months after GKRS (5.590 cm³), growth rate of 0.18%/m (Fig. 1F). ADC value of 996×10^{-6} mm²/s (Fig. 1G), very high FA value of 0.407 (Fig. 1H)

Longitudinal Diffusivity (LD) and Radial Diffusivity (RD) as well as b₀-images were calculated and exported. Using MRIcro, meningiomas were outlined in b₀-images. These regions of interest (ROIs) were placed on the parameter maps and DTI parameter values were calculated as described above (Fig. 1).

Parameters were correlated to a tumor volume change per natural logarithm of time, to account for the near-exponential decrease of tumor volume over time. During an initial

phase of 6 months after SRS, early imaging estimations of the tumor volume may not correlate with the final tumor response [30]. After this 6-months period, most meningiomas volumes follow an exponential trend, according to our data. To compare volume changes at different points in time, tumor volume change per natural logarithm of time is more accurate than volume change per time, particularly for long FU periods (FUP). Relative volume change per time was defined as the difference between tumor volume before SRS

and at last FU, related to initial tumor volume and the natural logarithm of the time interval between the date of SRS and last FU. The following formula was applied:

$$\text{Relative volume change per ln(month)} = \frac{\text{Volume at last FUP} - \text{Initial volume at SRS}}{\text{Initial Volume} * \ln(\text{FUP})}$$

Statistical analysis

While meningioma volume was measured before SRS and compared to volume at last FU, ADC and DTI parameters were measured before SRS (“parameter 1”) and at first follow-up (“parameter 2”). Differences between parameters 1 and 2 were calculated (“diff”). To compensate for the variation of first FU times (average 7.2 months, range 2.4 to 15.2 months), we related the difference between parameters 1 and 2 to time. To evaluate partial correlation, individual linear regression analyses were performed using relative volume change per ln(month) as the dependent variable and ADC and the following DTI parameters as independent variables: FA, MD, LD, and RD, each of them measured before SRS, at first FU and as difference, related to its initial value and the time interval between SRS and first FU.

Further, all analyses were corrected for age, gender, tumor volume before SRS, and the Paddick conformity index (PCI) as independent variables. These covariates were included in the regression models to adjust the results to reduce bias, as

they could pose potential confounding factors based on their biological plausibility.

All multiple linear regression statistical requirements were met in each analysis. There was linearity, as assessed by partial regression plots and a plot of studentized residuals against the predicted values; independence of residuals, as assessed by Durbin-Watson statistic tests; homoscedasticity, as assessed by visual inspection of a plot of studentized residuals versus unstandardized predicted values; no evidence of multicollinearity, as assessed by tolerance values greater than 0.1 and univariate Pearson correlations no greater than 0.4 for independent variables. There were no significant outliers assessed by no studentized deleted residuals greater than ± 3 standard deviations, no leverage values greater than 0.25, no values for Cook’s distance above 1, and no multivariate outliers based on Mahalanobis distance analyses. The assumption of normality was met, as assessed by a Q–Q Plot and histogram visual inspection of standardized residuals.

A p -value ≤ 0.05 was considered as a nominal statistical significance. All analyses were performed using SPSS v.26.0 [31].

Results

After a mean FUP of 52.7 months, 69 of 70 meningiomas were controlled (control rate 98.6%), with a mean volume reduction of 34.9%.

Table 3 Multivariate linear regression analysis results for Difference of Volume/ln(T) as dependent variable

Parameter	Mean \pm SD	Stand. β	Partial correlation	p value	Adjusted R^2
ADC 1 10^{-6} mm ² /s	932.37 \pm 150.39	− 0.275	− 0.292	0.029	0.205**
ADC 2 10^{-6} mm ² /s	1004.85 \pm 221.641801	0.045	0.043	0.750	0.074
Diff. ADC (%)	− 0.010263 \pm 0.025096	− 0.291	− 0.292	0.034	0.154*
FA 1	0.245964 \pm 0.070471	− 0.562	− 0.607	0.000001	0.443***
FA 2	0.245506 \pm 0.068135	− 0.348	− 0.358	0.006	0.184**
Diff. FA (%)	− 0.005005 \pm 0.031005	− 0.418	− 0.404	0.002	0.260**
MD 1 (mm ² /s)	0.000956 \pm 0.000231	− 0.263	− 0.283	0.047	0.205**
MD 2 (mm ² /s)	0.001040 \pm 0.000269	− 0.044	− 0.045	0.743	0.086
Diff. MD (%)	− 0.012515 \pm 0.022925	− 0.070	− 0.074	0.619	0.086
LD 1 (mm ² /s) (s/mm ²)	0.001159 \pm 0.000291	− 0.341	− 0.375	0.007	0.270**
LD 2 (mm ² /s)	0.001262 \pm 0.000295	− 0.030	− 0.031	0.820	0.085
Diff. LD (%)	− 0.010438 \pm 0.021415	− 0.297	− 0.319	0.031	0.176*
RD 1 (mm ² /s)	0.000845 \pm 0.000221	− 0.143	− 0.155	0.277	0.169*
RD 2 (mm ² /s)	0.000939 \pm 0.000277	− 0.030	− 0.032	0.810	0.065
Diff. RD (%)	− 0.017556 \pm 0.029120	0.220	0.240	0.104	0.134*

Model = “Enter” method in SPSS Statistics; DeltaVolume/ln(T) = Volume change per ln(month); Adjusted R^2 = Adjusted coefficient of determination of regression model; Stand. β = Standardized Coefficient of determination; All individual analyses of each parameter were adjusted by the same covariables: age, gender, volume of tumor before SRS and Paddick conformity index.

* $p < 0.05$. ** $p < 0.01$. *** $p < 0.001$

Whereas FA values of the initial exam showed the highest correlation to tumor volume change at the last FU (Correlation Coefficient $CC = -0.607$), followed by the differences between the first and the second FU value of FA ($CC = -0.404$) and the first LD value ($CC = -0.375$), the CC s of all ADC values were comparably low ($CC = -0.292$ for ADC1, $CC = -0.043$ for ADC2 and $CC = -0.292$ for the difference between the two ADC values). Nevertheless, all these correlations, except for ADC2 values, reached significance. The correlations of MD and RD values were lower than those of FA and LD, the highest being MD1 with $CC = -0.283$ (Table 3).

All three cases presenting tumor volume increase showed FA1 values above the mean FA1 value plus one standard deviation, which amounts to $FA_{lim} = 0.3164$. Additionally, 6 cases without progression were found above this value. Therefore taking $FA_{lim} = 0.3164$ as a threshold, the positive predictive value for tumor progression was 100%, and the negative predictive value was 96.5%, with a relatively low sensitivity of 33.3%, according to MedCalc Diagnostic Test Program (www.medcalc.org/calc/diagnostic_test.php).

The receiver operating characteristic (ROC) curve for the predictive power of pre-GKRS FA-values, with a cutoff for meningioma regression defined as 1.0% volume reduction per month, yielded an area under the curve (AUC) = 0.88 (Fig. 2).

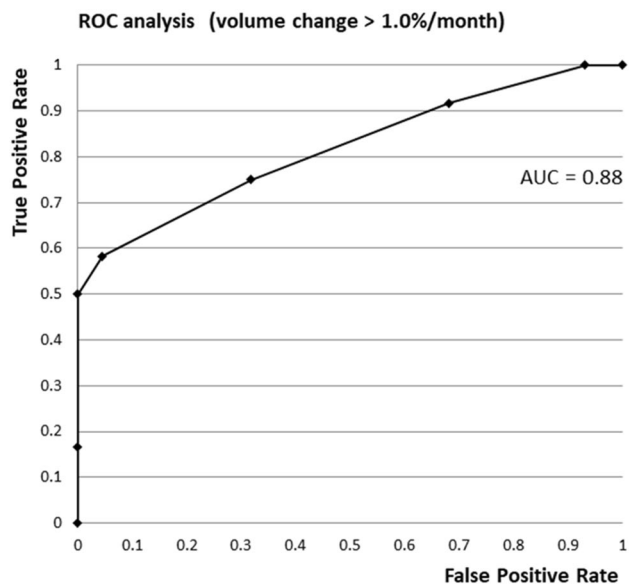


Fig. 2 Receiver operating characteristic (ROC) curve for the predictive power of pre GKRS FA-values, with cutoff for meningioma regression defined as 1.0% volume reduction per month, yielded an area under the curve (AUC) = 0.88

Discussion

For the first time, the prognostic value of ADC maps measured in meningiomas before and shortly after SRS was compared to simultaneously acquired DTI parameter maps. As described in the results section, values taken from ADC maps do not correlate as well as the DTI-parameter FA to volumetric treatment response. In another study of meningiomas, a moderated correlation was found similarly: ADC mean value correlated negatively with tumor proliferation index Ki 67, but only the minimum of these ADC values correlated with tumor cell count [32].

This result is in line with our previous analysis, where MD, among other parameters, correlated significantly but to a lesser degree than FA to late volume changes [22]. Similar to ADC, MD is the sum of the scalar invariants—divided by three—from the three diffusion tensor eigenvalues measured on a voxelwise basis. It represents a tissue parameter and does not depend on the orientation of patients, the magnetic field, or gradient directions. In contrast, mainly in white matter, ADC measurement is not entirely independent from the primary fiber orientation [33].

In extracerebral tumors, pretreatment ADC has been used to predict radiation response in vestibular schwannomas [34]. In meningiomas, ADC values were significantly lower in those tumors which did not show progression or recurrences after an operation with or without adjuvant radiotherapy [35]. After proton therapy of meningiomas, ADC values increased progressively with a peak at three months in well-responding tumors. In contrast, the group with less volume reduction, which had exhibited higher pretreatment ADC values, reached its peak ADC values at 12–15 months and then progressively decreased [36]. Intravoxel incoherent motion imaging (IVIM) was used to detect early microstructural changes after proton therapy. Whereas post-treatment ADC changes did not correlate significantly to volume reduction, “true” diffusion values after correction for the “pseudo-diffusion” fraction, which is due to the random movement of blood within capillaries, corresponded well to tumor shrinkage [37]. This technique of “true diffusion imaging” however, was not available to us.

A differentiation between typical and atypical meningiomas based on ADC values, as reported by Yin et al. [38], was not the subject of the present study. We deliberately included only low-grade meningiomas, at least according to imaging criteria, to keep the group as homogeneous as possible. Thus, our results only apply to WHO grade I meningiomas and not to those where a higher grade is suspected.

In the imaging of intracerebral tumors, the reverse relation of ADC value and cellularity has been used to predict the grading of gliomas and to differentiate them from metastases and lymphomas [39–41]. However, according to meta-analysis results, cellularity and ADC value do not correlate in all neoplasms as well as in gliomas because other factors

may be involved as the extracellular matrix, nucleic acids, ratio of stroma/parenchyma and microvessel density as well as changes in susceptibility due to hemorrhages, etc. [42, 43]

The course of ADC values measured at close follow-ups after treatment has been used to monitor the progression of tissue response of neoplasms in general [44]. The effects of radiation are not limited to direct cell death but include vascular disruption and consequently, hypoperfusion and edema, additionally inflammatory response, finally resulting in decreased vascularity and fibrosis [45, 46]. Following radiation, ADC may decrease transiently due to cell swelling before it finally increases due to cell death in responding brain metastases and thus allows for early stratification of radiotherapy [47]. Thus, high ADC values measured during follow-up have been used as well to differentiate radiation injury characterized by gliosis and cell death from recurrence in high-grade gliomas [48]. In meningiomas however, Berberat et al. [13] observed no significant changes in long-term FU ADC values after SRS and reported a progression rate of 16.7%. However, this study did not distinguish between meningioma grades and possibly included meningiomas of a higher grade.

We limited our study to WHO grade I meningiomas, mainly established on imaging criteria, as only for nine cases were we able to retrieve histology results. The relatively short FUP and the retrospective design of the prognostic models were further limitations.

Conclusion

For the first time, the prognostic value of ADC maps measured in meningiomas before and shortly after Gamma Knife SRS is compared to simultaneously acquired DTI parameter maps. According to our results, quantities assessed from ADC maps present significant correlations to the volumetric meningioma response. However, they are less effective than correlations with several DTI-derived parameters, particularly the Fractional Anisotropy, which reaches an AUC value of 0.88. Because of the much higher correlation of DTI parameters with meningioma shrinkage, we cannot recommend replacing FA as a successful predictor with parameters measured from simple DWI.

Author contributions Conception and design: HS and PS, Data collection: All authors, Data analysis and interpretation: HS, SPS, RMG, PS, Manuscript writing: HS, SPS, RMG, PS, All authors reviewed the manuscript.

Funding This study has not received any financial support.

Data availability The datasets generated during and analyzed during the current study are available from the corresponding author on reasonable request.

Declarations

Conflict of interest The authors have no personal, financial, or institutional interest in any of the drugs, materials, or devices described in this article.

References

1. Rogers L, Barani I, Chamberlain M, Kaley TJ, McDermott M, Raizer J et al (2015) Meningiomas: knowledge base, treatment outcomes, and uncertainties. *A RANO rev J Neurosurg* 122(1):4–23
2. Cohen-Inbar O, Lee CC, Sheehan JP (2016) The contemporary role of stereotactic radiosurgery in the treatment of meningiomas. *Neurosurg Clin N Am* 27(2):215–28
3. Ius T, Tel A, Minniti G, Somma T, Solari D, Longhi M et al (2021) Advances in multidisciplinary management of skull base meningiomas. *Cancers (Basel)* 13(11):2664
4. Sheehan J, Pikis S, Islim AI, Chen CJ, Bunevicius A, Peker S et al (2022) An international multicenter matched cohort analysis of incidental meningioma progression during active surveillance or after stereotactic radiosurgery: the IMPASSE study. *Neuro Oncol* 24(1):116–124
5. Fatima N, Meola A, Pollom E, Chaudhary N, Soltys S, Chang SD (2019) Stereotactic radiosurgery in large intracranial meningiomas: a systematic review. *World Neurosurg* 129:269–275
6. Helis CA, Hughes RT, Cramer CK, Tatter SB, Laxton AW, Bourland JD et al (2020) Stereotactic radiosurgery for atypical and anaplastic meningiomas. *World Neurosurg* 144:e53–61
7. DiBiase SJ, Kwok Y, Yovino S, Arena C, Naqvi S, Temple R et al (2004) Factors predicting local tumor control after gamma knife stereotactic radiosurgery for benign intracranial meningiomas. *Int J Radiat Oncol Biol Phys* 60(5):1515–9
8. Starke RM, Nguyen JH, Rainey J, Williams BJ, Sherman JH, Savage J et al (2011) Gamma Knife surgery of meningiomas located in the posterior fossa: factors predictive of outcome and remission. *J Neurosurg* 114(5):1399–1409
9. Santacrose A, Walier M, Régis J, Liščák R, Motti E, Lindquist C et al (2012) Long-term tumor control of benign intracranial meningiomas after radiosurgery in a series of 4565 patients. *Neurosurgery* 70(1):32–39
10. Sheehan JP, Starke RM, Kano H, Kaufmann AM, Mathieu D, Zeiler FA et al (2014) Gamma knife radiosurgery for sellar and parasellar meningiomas: a multicenter study. *J Neurosurg* 120(6):1268–1277
11. Mansouri A, Larjani S, Klironomos G, Laperriere N, Cusimano M, Gentili F et al (2015) Predictors of response to gamma knife radiosurgery for intracranial meningiomas. *J Neurosurg* 123(5):1294–1300
12. Speckter H, Radulovic M, Trivodaliev K, Vranes V, Joaquin J, Hernandez W et al (2022) MRI radiomics in the prediction of the volumetric response in meningiomas after gamma knife radiosurgery. *J Neurooncol* 159(2):281–291
13. Filippi CG, Edgar MA, Uluğ AM, Prowda JC, Heier LA, Zimmerman RD (2001) Appearance of meningiomas on diffusion-weighted images: correlating diffusion constants with histopathologic findings. *AJNR Am J Neuroradiol* 22(1):65–72
14. Kashimura H, Inoue T, Ogasawara K, Arai H, Otawara Y, Kanbara Y et al (2007) Prediction of meningioma consistency using fractional anisotropy value measured by magnetic resonance imaging. *J Neurosurg* 107:784–787
15. Tropine A, Dellani PD, Glaser M, Bohl J, Plöner T, Vucurevic G et al (2007) Differentiation of fibroblastic meningiomas from other

- benign subtypes using diffusion tensor imaging. *J Magn Reson Imaging* 25(4):703–708
16. Yan PF, Yan L, Hu TT, Xiao DD, Zhang Z, Zhao HY et al (2017) The potential value of preoperative mri texture and shape analysis in grading meningiomas: a preliminary investigation. *Transl Oncol* 10(4):570–577
 17. Coroller TP, Bi WL, Huynh E, Abedalthagafi M, Aizer AA, Greenwald NF et al (2017) Radiographic prediction of meningioma grade by semantic and radiomic features. *PLoS ONE* 12(11):e0187908
 18. Hale AT, Stonko DP, Wang L, Strother MK, Chambless LB (2018) Machine learning analyses can differentiate meningioma grade by features on magnetic resonance imaging. *Neurosurg Focus* 45(5):E4
 19. Kalasauskas D, Kronfeld A, Renovanz M, Kurz E, Leukel P, Krenzlin H et al (2020) Identification of high-risk atypical meningiomas according to semantic and radiomic features. *Cancers (Basel)* 12(10):2942
 20. Speckter H, Bido J, Hernandez G, Mejía DR, Suazo L, Valenzuela S et al (2016) Prognostic value of diffusion tensor imaging parameters for Gamma Knife radiosurgery in meningiomas. *J Neurosurg* 125(Supplement_1):83–88
 21. Berberat J, Roelcke U, Remonda L, Schwyzer L (2021) Long-term apparent diffusion coefficient value changes in patients undergoing radiosurgical treatment of meningiomas. *Acta Neurochir (Wien)* 163(1):89–95
 22. Speckter H, Bido J, Hernandez G, Rivera D, Suazo L, Valenzuela S et al (2018) Pretreatment texture analysis of routine MR images and shape analysis of the diffusion tensor for prediction of volumetric response after radiosurgery for meningioma. *J Neurosurg* 129(Suppl1):31–37
 23. Changizi V, Kadhum MJ, Taher HJ, Najim HS, Saroush HA (2021) Grading meningiomas by used imaging features on magnetic resonance imaging. *Clin Schizophr Relat Psychoses*. <https://doi.org/10.3371/CSRP.CVKM.081221>
 24. Patibandla MR, Lee CC, Tata A, Addagada GC, Sheehan JP (2018) Stereotactic radiosurgery for WHO grade I posterior fossa meningiomas: long-term outcomes with volumetric evaluation. *J Neurosurg* 129(5):1249–1259
 25. McMahon SJ (2018) The linear quadratic model: usage, interpretation and challenges. *Phys Med Biol* 64(1):01TR01
 26. Speckter H, Santana J, Miches I, Hernandez G, Bido J, Rivera D et al (2019) Assessment of the alpha/beta ratio of the optic pathway to adjust hypofractionated stereotactic radiosurgery regimens for perioptic lesions. *J Radiat Oncol* 8(3):279–289
 27. Vernimmen FJAI, Slabbert JP (2010) Assessment of the α/β ratios for arteriovenous malformations, meningiomas, acoustic neuromas, and the optic chiasma. *Int J Radiat Biol* 86(6):486–498
 28. Piper K, Yu S, Taghvaei M, Fernandez C, Mouchtouris N, Smit RD, Yudkoff C, Collopy S, Reyes M, Lavergne P, Karsy M, Prashant GN, Shi W, Evans J (2022) Radiation of meningioma dural tail may not improve tumor control rates. *Front Surg* 9:908745. <https://doi.org/10.3389/fsurg.2022.908745>. (PMID: 35860199; PMCID: PMC9289604)
 29. Huang RY, Bi WL, Weller M, Kaley T, Blakeley J, Dunn I et al (2019) Proposed response assessment and endpoints for meningioma clinical trials: report from the response assessment in neuro-oncology working group. *Neuro Oncol* 21(1):26–36
 30. Harrison G, Kano H, Lunsford D, Flickinger JC, Kondziolka D (2015) Quantitative tumor volume responses after Gamma Knife radiosurgery for meningiomas. *J Neurosurg* 124:146–154
 31. Corporation IBM (2019) SPSS statistics for Windows. Armonk, NY
 32. Surov A, Gottschling S, Mawrin C, Prell J, Spielmann RP, Wienke A et al (2015) Diffusion-weighted imaging in meningioma: prediction of tumor grade and association with histopathological parameters. *Transl Oncol* 8(6):517–523
 33. Winston GP (2012) The physical and biological basis of quantitative parameters derived from diffusion MRI. *Quant Imaging Med Surg* 2(4):254–265
 34. Camargo A, Schneider T, Liu L, Pakpoor J, Kleinberg L, Yousem DM (2017) Pretreatment ADC values predict response to radiosurgery in vestibular schwannomas. *Am J Neuroradiol* 38(6):1200–1205
 35. Ko CC, Zhang Y, Chen JH, Chang KT, Chen TY, Lim SW et al (2021) Preoperative MRI radiomics for the prediction of progression and recurrence in meningiomas. *Front Neurol* 12:636235
 36. Feraco P, Scartoni D, Porretti G, Pertile R, Donner D, Picori L et al (2021) Predict treatment response by magnetic resonance diffusion weighted imaging: a preliminary study on 46 meningiomas treated with proton-therapy. *Diagnostics* 11(9):1684
 37. Franconeri A, Sacco S, Raciti MV, Maggi A, Muzic SI, Imparato S et al (2021) Intravoxel incoherent motion as a tool to detect early microstructural changes in meningiomas treated with proton therapy. *Neuroradiology* 63(7):1053–1060
 38. Yin B, Liu L, Zhang BY, Li YX, Li Y, Geng DY (2012) Correlating apparent diffusion coefficients with histopathologic findings on meningiomas. *Eur J Radiol* 81(12):4050–4056
 39. Cha S (2006) Update on brain tumor imaging: from anatomy to physiology. *AJNR Am J Neuroradiol* 27:475–487
 40. Lin X, Lee M, Buck O, Woo KM, Zhang Z, Hatzoglou V et al (2017) Diagnostic accuracy of T1-weighted dynamic contrast-enhanced-MRI and DWI-ADC for differentiation of glioblastoma and primary CNS lymphoma. *Am J Neuroradiol* 38(3):485–491
 41. Drake-Pérez M, Boto J, Fitsiori A, Lovblad K, Vargas MI (2018) Clinical applications of diffusion weighted imaging in neuroradiology. *Insights Imaging* 9(4):535–547
 42. Schwyzer L, Berberat J, Remonda L, Roelcke U (2015) Susceptibility changes in meningiomas influence the apparent diffusion coefficient in diffusion-weighted MRI. *J Neuroradiol* 42(6):332–337
 43. Surov A, Meyer HJ, Wienke A (2017) Correlation between apparent diffusion coefficient (ADC) and cellularity is different in several tumors: a meta-analysis. *Oncotarget* 8(35):59492–59499
 44. Campbell A, Davis LM, Wilkinson SK, Hesketh RL (2019) Emerging functional imaging biomarkers of tumour responses to radiotherapy. *Cancers (Basel)* 11(2):131
 45. Eriksson D, Stigbrand T (2010) Radiation-induced cell death mechanisms. *Tumor Biol* 31(4):363–372
 46. Barker HE, Paget JTE, Khan AA, Harrington KJ (2015) The tumour microenvironment after radiotherapy: mechanisms of resistance and recurrence. *Nat Rev Cancer* 15(7):409–425
 47. Mahmood F, Johannesen HH, Geertsen P, Hansen RH (2017) Repeated diffusion MRI reveals earliest time point for stratification of radiotherapy response in brain metastases. *Phys Med Biol* 62(8):2990–3002
 48. Hein PA, Eskey CJ, Dunn JF, Hug EB (2004) Diffusion-weighted imaging in the follow-up of treated high-grade gliomas: tumor recurrence versus radiation injury. *AJNR Am J Neuroradiol* 25:201–209

Publisher's Note Springer Nature remains neutral with regard to jurisdictional claims in published maps and institutional affiliations.

Springer Nature or its licensor (e.g. a society or other partner) holds exclusive rights to this article under a publishing agreement with the author(s) or other rightsholder(s); author self-archiving of the accepted manuscript version of this article is solely governed by the terms of such publishing agreement and applicable law.